

Dynamic Model Identification for Industrial Robots

JAN SWEVERS, WALTER VERDONCK, and JORIS DE SCHUTTER

INTEGRATED EXPERIMENT DESIGN AND PARAMETER ESTIMATION

Industrial robot manipulators are indispensable for achieving productivity and flexibility in fully automated production lines, where they are used for a wide variety of tasks, ranging from material handling and assembly to cutting, welding, gluing, and painting. To improve productivity and accuracy, robot manufacturers invest time and effort in developing advanced offline programming tools and controllers. Dynamic robot models are a key element in these developments.

OFFLINE PROGRAMMING AND TASK OPTIMIZATION

In industrial practice, many robots are programmed manually by leading the robot through a sequence of position points. This approach, known as online programming, has the advantage that positions defined by task execution are more accurate than a path specified in a software environment. On the other hand, online programming requires idle time that may be unacceptable in the case of small product batch sizes.

Robot setup times can be kept short if the task is programmed without interrupting the production process. This approach, known as offline programming, occurs in a software

Digital Object Identifier 10.1109/MCS.2007.904659

occurs in a software

environment. Many robot manufacturers, such as KUKA, ABB, and Fanuc, as well as third-party companies, offer software for offline programming. These interactive simulation environments allow the user to create virtual models of production environments and to program and simulate robot manipulator tasks before transferring the code to the robot controller (Figure 1). In particular, three-dimensional graphics are used to coordinate the elements of the production process and detect possible collisions and other system failures.

Offline programming software does not consider uncertainty in the position and orientation of the objects in the production environment. In addition, it is assumed that the robot manipulator executes the programmed task with perfect position accuracy. However, the trajectories executed by the robot manipulator in practice differ significantly from the programmed and simulated trajectories due to kinematic modeling errors and robot dynamics. Inaccuracies due to kinematic errors can be compensated for by using a calibrated kinematic model of the robot manipulator [1]. However, for high-speed motions, or in case of a heavy payload, the tracking error is caused mainly by dynamic forces, for example, centrifugal and Coriolis forces, dynamic coupling between the joint axes, and actuator dynamics. These effects are not sufficiently accounted for by standard industrial robot controllers. Dynamic effects can be compensated, however, by switching to more advanced model-based controllers or by adapting the programmed robot trajectory. In the latter case, the offline programming environment must include dynamic robot models as well as dynamic simulation functionality.

Another objective of offline programming is to minimize the cycle time of a robot task, since shorter cycle times lead to higher productivity. However, physical constraints, such as maximum motor and gearbox torques as well as maximum motor speeds, must be accounted for to avoid overload, which causes accelerated wear and tear of the actuators, gears, and bearings, resulting in loss of accuracy and even premature failure. Realistic simulation and optimization of the motion of a robot manipulator, including its physical constraints, requires an accurate dynamic model.

Advanced Robot Control

Standard industrial robot controllers consist of independent proportional-integral-differential (PID)-like position controllers, one for each joint. Although these controllers yield sufficiently accurate path tracking for most industrial applications, applications such as laser welding and laser cutting require higher accuracy. These applications are characterized by complex six-degree-of-freedom trajectories, fast motion, and stringent path-tracking accuracy requirements. Fast motion results in high dynamic coupling between the various robot links, which cannot be compensated for by a standard robot controller. Consequently, advanced robot

controllers have been developed, for example, computed-torque control as well as feedforward dynamic compensation [2]–[5]. These controllers are more complex than standard industrial robot controllers since they are based on a model of the complete robot dynamics. Although practical industrial conditions are far from those in laboratory environments, results obtained on industrial setups confirm the benefits of model-based control [6]. Improved tracking accuracy is obtained, provided that the robot model is sufficiently accurate for torque prediction.

INTEGRATED EXPERIMENTAL ROBOT IDENTIFICATION

A dynamic robot model, which relates robot motion to joint torques, describes the rigid-body dynamics of the robot and includes Coulomb and viscous friction in the joints. Although inertia estimates can be derived from CAD drawings, robot manufacturers do not provide these drawings for all parts of the robot, for example, parts manufactured by external suppliers. Dismantling the robot to measure mass and inertia properties of the links is not a realistic option. Moreover, estimates of friction parameters are not provided by the manufacturers and are not predictable from first principles.

Experimental identification using motion and torque data measured during experiments is thus needed to obtain accurate estimates of robot model parameters. In particular, we present an experimental robot identification procedure based on the maximum likelihood framework with periodic bandlimited excitation [7].

The input to the identification procedure is kinematic and geometric information about the robot manipulator, as well as specifications about the desired model accuracy; see

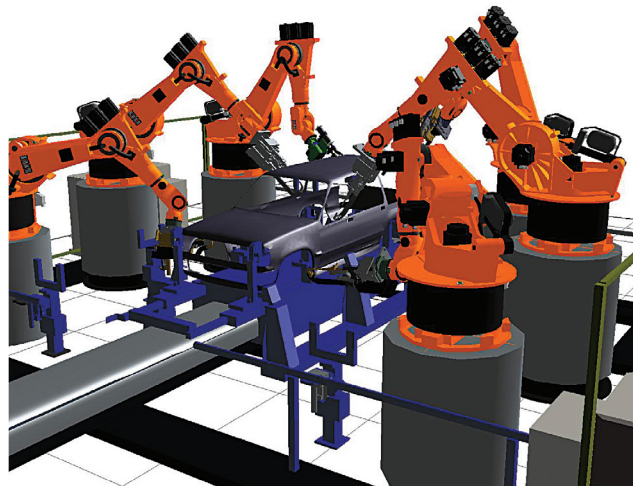


FIGURE 1 Illustrative graphical output of the KUKA offline programming environment KUKASim. A complete production process can be simulated in a virtual environment, collisions can be detected, and robot programs can be generated automatically. Cycle-time optimization is possible but is limited to geometric and kinematic information. (Courtesy of KUKA.)

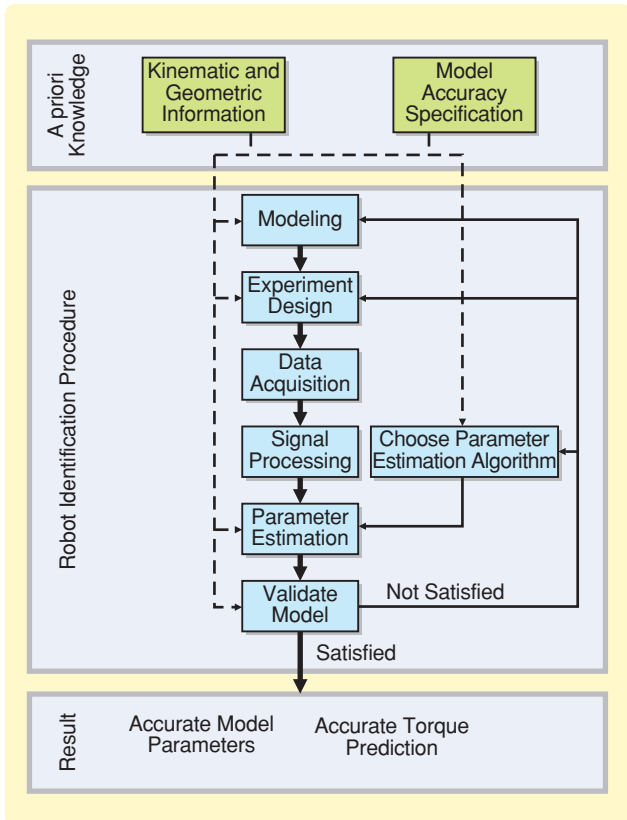


FIGURE 2 Schematic representation of a standard experimental robot identification procedure. The kinematic and geometric information of the robot manipulator and model-accuracy specifications are the inputs to the identification procedure. This information is available prior to the identification and determines choices to be made in the procedure. The model validation step evaluates the accuracy of the model according to criteria that depend on the application of the model. If the identified model does not pass the validation tests, one or several steps of the procedure are repeated and choices are reconsidered.

Figure 2. These inputs determine the choices to be made in the procedure. For example, kinematic and geometric information about the robot includes the number of joints, the orientations of the joint axes, and the lengths of the robot links. Model accuracy specifications determine the type of model to be used and the level of detail of the dynamics to be included in the model. These choices have implications for the various steps of the identification procedure.

The last step of the identification procedure is model validation, where the user verifies that the model satisfies the accuracy specifications. If the obtained model does not pass the validation tests, one or several steps of the procedure are repeated and some of the choices are reconsidered.

MODELING

Dynamic robot models define the relationship between the motion of the robot manipulator and the actuator torques. The motion of the robot is described by the position, velocity, and acceleration of all of its links. The robot is repre-

sented by a kinematic chain of rigid bodies, and thus rigid-body dynamic equations are the basis for the model. Depending on the system and on the specifications, these rigid-body equations have to be complemented with models of other effects such as friction and gravity-compensating devices if present.

Rigid-Body Dynamics

The Newton-Euler or Lagrangian method is used to derive the dynamic equations of kinematic chains of rigid bodies [8]. Both approaches yield the dynamics equation

$$\tau = M(q, \vartheta) \ddot{q} + C(q, \dot{q}, \vartheta) + g(q, \vartheta), \quad (1)$$

which expresses, for an n -degree-of-freedom robot, the n -vector of actuator torques τ as a function of the n -vectors of the joint positions q , velocities \dot{q} , and accelerations \ddot{q} as well as the model parameters ϑ . In (1), $M(q, \vartheta)$ is the $n \times n$ inertia matrix, $C(q, \dot{q}, \vartheta)$ is the n -vector containing Coriolis and centrifugal forces, and $g(q, \vartheta)$ represents gravitational torques. $M(q, \vartheta)$, $C(q, \dot{q}, \vartheta)$, and $g(q, \vartheta)$ are nonlinear functions of the model parameters ϑ , that is, the mass, center-of-gravity location, and moments and products of inertia of each link.

Using the barycentric parameters [9] or the modified Newton-Euler parameters [8] yields a model of the form

$$\tau = \Phi(q, \dot{q}, \ddot{q}) \theta, \quad (2)$$

which is linear in the unknown parameters. In (2), θ is the barycentric parameter vector, and Φ is the observation or identification matrix, which depends only on the motion data. This property simplifies the parameter estimation considerably [10]. The barycentric parameters of a link are combinations of the inertial parameters of the link and its descendants in the kinematic chain [11]. For example, the barycentric mass of a link is defined as the mass of that link augmented by the total mass of all descendant links. The modified Newton-Euler parameters express the inertial parameters as first- and second-order moments with respect to a link frame located at the joint axis.

Gravity Compensation, Dynamic Coupling, and Friction

Rigid-body equations (1) and (2) include only the effects of link masses and inertias. Friction, dynamic coupling due to the inertia of geared actuator rotors that spin at high velocity [12], as well as the effects of gravity-compensating devices if present contribute significantly to the dynamic behavior of the robot manipulator. Gravity-compensating devices, which are preloaded springs mounted between the first and second link, approximately compensate the static torque caused by the mass of the payload and robot wrist on the actuator of the second link, that is, the shoulder actuator [13]. Dynamic coupling and gravity-compensating springs can be described by mathematical

Periodic excitation allows us to integrate the experiment design, signal processing, and parameter estimation.

expressions that are linear in the parameters. Consequently, these effects fit conveniently within the linear-in-parameters model structure (2).

Although friction is a complex nonlinear phenomenon, especially during motion reversal [14], [15], a friction model consisting of only Coulomb and viscous friction, that is,

$$\tau_{fric} = f_c \text{sign}(\dot{q}) + f_v \dot{q}, \quad (3)$$

is an acceptable simplification for many robotics applications [16]. Note that (3) is linear in the unknown Coulomb and viscous friction parameters f_c and f_v and thus is consistent with the linear model structure (2).

EXPERIMENT DESIGN

During the design of an identification experiment, it is necessary to ensure that the excitation is sufficient to provide accurate and fast parameter estimation in the presence of disturbances, and that the processing of the resulting data is simple and yields accurate results. The experiment design consists of two steps. First, a trajectory parameterization is selected, and second the trajectory parameters are calculated, usually by means of optimization.

Trajectory Parameterization

Several approaches exist for parameterizing robot-excitation trajectories, for example, finite sequences of joint accelerations [17], or fifth-order polynomials interpolating between sets of joint positions and velocities separated in time [18]. Although these trajectories provide adequate excitation of the robot dynamics, the resulting measurement data are neither periodic nor bandlimited. Processing periodic, bandlimited measurements is more accurate, simplifying and improving the accuracy of the parameter estimates.

Periodic bandlimited measurements are obtained if the excitation is periodic and bandlimited, that is, if the trajectory $q_i(t)$ of each joint i is periodic, parameterized as a finite Fourier series

$$q_i(t) = q_{i,0} + \sum_{k=1}^N (a_{i,k} \sin(k\omega_f t) + b_{i,k} \cos(k\omega_f t)), \quad (4)$$

where t represents time, and ω_f is the same for all joints. This Fourier series is periodic with period $T_f = 2\pi/\omega_f$, which is chosen to be an integer multiple of the sampling period. Each Fourier series contains $2N + 1$ parameters, which are the degrees of freedom for trajectory optimiza-

tion. The coefficients $a_{i,k}$ and $b_{i,k}$ are the amplitudes of the sine and cosine functions along with the offset $q_{i,0}$ of the position trajectory.

In choosing the frequency range $[\omega_f, N\omega_f]$ of the excitation trajectories, the following trade-off has to be considered. By selecting a low fundamental frequency ω_f , that is, a long excitation period, a larger part of the robot workspace can be covered for given maximum joint velocities, however, at the cost of longer measurement time. Good coverage of the robot workspace improves the information content of the measurements as well as the accuracy of the parameter estimates [19]. On the other hand, including high frequencies provides high accelerations, which are required to accurately estimate the moments and products of inertia. The highest frequency of the commanded trajectory, however, is limited by the lowest resonance frequency of the robot structure. The structural flexibilities of the robot are excited if the highest frequencies of the trajectory are too close to the lowest resonance frequency. Excitation of flexible modes is disadvantageous because they are not accounted for in the rigid-body robot model. As discussed below, the commanded trajectory need not be followed exactly since the actual motion of the robot is measured.

Trajectory Optimization

Appropriate values for the trajectory parameters can be selected either by trial and error or by solving a nonlinear optimization problem with constraints imposed on the robot motion.

Several objective functions exist for trajectory optimization. A popular optimization criterion is the logarithm of the determinant of the covariance matrix of the model parameter estimates, known as the *d-optimality* criterion [10]. This criterion measures the size of the uncertainty region of the model parameter estimates. Its calculation does not depend on the model parameters if the joint position, velocity, and acceleration data are free of noise but rather depends only on the robot trajectory through the identification matrix Φ in (2) as well as on the covariance of the noise on the actuator torque measurements [20]. This property is useful in practice since the optimization of the robot excitation can be performed without any prior knowledge of the model parameters.

The motion constraints impose limitations on the joint positions, velocities, and accelerations as well as on the robot end-effector position in Cartesian space. These limitations avoid collisions between the robot and objects in its environment as well as collisions between robot links.

Online programming has the advantage that positions defined by task execution are more accurate than a path specified in a software environment.

ROBOT EXCITATION, DATA ACQUISITION, AND SIGNAL PROCESSING

The optimized robot-excitation trajectory is programmed in the robot controller. The robot repeats the trajectory continuously, while data are collected at a constant, user-specified sampling frequency. Data collection starts after the transient response caused by the startup of the experiment dies out.

Joint positions are measured using encoders mounted on the actuator shafts. Since the measured joint trajectories deviate from the desired trajectories, due to the limitations of the robot controller, the measured joint positions are used for parameter estimation instead of the

commanded trajectories. Although these measurements may contain more or different harmonics than the commanded trajectories, the motion is periodic, with the same period as that of the commanded trajectories, and bandlimited, because the robot is controlled by a bandlimited position-feedback controller.

The actuator torque data are obtained through actuator current measurements without additional sensors. The relationship between current and torque is modeled as linear or as a higher order polynomial [21], of which the parameters are provided by the motor manufacturer or identified in a separate experiment [22].

The aim of the signal processing step is to clean up the measured data. This step improves the signal-to-noise ratio of torque and joint position measurements, estimates the variance of the measurement noise, and calculates the joint velocity and acceleration estimates based on the measured joint positions.

Data Averaging and Noise Variance Estimation

Measurement noise, which is assumed to be an additive normally distributed zero-mean stochastic disturbance, causes uncertainty and bias errors in the parameter estimates. For a given data set, bias errors can be avoided and uncertainty can be minimized by using an efficient estimator, for example, a maximum likelihood estimator. This estimator yields unbiased parameter estimates with minimal uncertainty when correct values for the noise covariance are used [19, pp. 20–25] and [23, pp. 92–106].

Since the data are periodic, the signal-to-noise ratio can be improved by data averaging without using a lowpass noise filter. Averaging, which is used by all spectrum analyzers, improves the quality of the data with the square root of the number of measured periods.

To estimate the noise level on measured periodic signals, the sample variance of a signal x consisting of M periods of K samples is given by

$$\sigma_x^2 = \frac{1}{(MK - 1)} \sum_{k=1}^K \sum_{m=1}^M (x_m(k) - \bar{x}(k))^2, \quad (5)$$

where $x_m(k)$ indicates the k th sample within the m th period, and $\bar{x}(k)$ denotes the average of x , that is,

$$\bar{x}(k) = \frac{1}{M} \sum_{m=1}^M x_m(k). \quad (6)$$

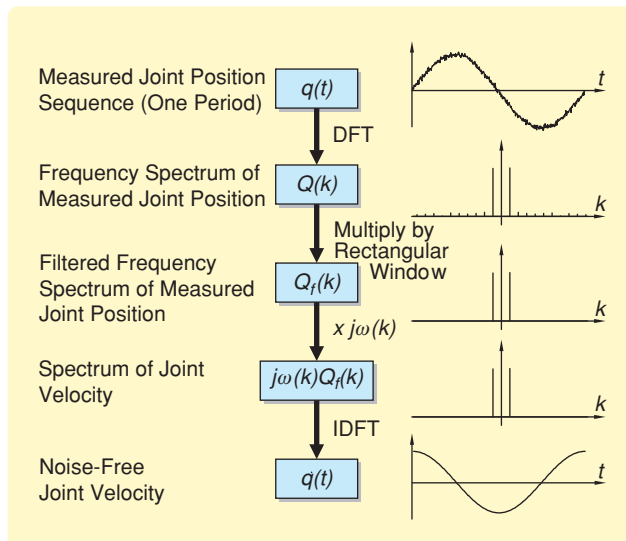


FIGURE 3 Exact frequency-domain differentiation of a measured periodic joint position signal. The left column explains the various steps of the procedure. The right column illustrates these steps for a periodic signal containing only one frequency, that is, a sinusoidal signal, perturbed with additive normally distributed noise. First, the signal is transformed to the frequency domain using the discrete Fourier transform (DFT). Next, the spectrum is multiplied by a rectangular window, which selects the frequencies that contain signal information. For this example, the multiplication corresponds to selecting one frequency. The spectrum is set to zero at all other frequencies. The resulting spectrum is then multiplied by the continuous-time frequency-domain representation of a differentiator at the selected frequency. That is, the spectrum is multiplied by $j\omega(k) = j2\pi kf_s/P$, with f_s the sampling frequency, P the number of time-domain samples, $k = \{-1, 1\}$ is the index of the selected frequency in the discrete spectrum. A transformation back into the time domain using the inverse DFT yields an estimate of the first time derivative of the original signal, that is, the velocity. The velocity signal is almost free of noise, that is, noise is removed from all frequencies except the selected ones. For simplicity, only the amplitude spectra are shown.

For robot identification the signal x corresponds to the measured actuator torques τ and joint positions q .

Exact Calculation of the Joint Velocities and Accelerations

Calculation of the identification matrix Φ given by (2) requires estimates of the joint velocities and accelerations. Numerical differentiation amplifies the noise present in the measurements, while noisy joint velocity and acceleration estimates deteriorate the accuracy of the parameter estimates.

Exact differentiation is possible when the joint position measurements are periodic, bandlimited, and the sampling frequency f_s is at least twice the bandwidth to avoid aliasing. To calculate the joint velocities and accelerations, the averaged joint position measurements are transformed to the frequency domain using the discrete Fourier transform. This transformation does not introduce leakage errors if an integer number of periods is selected. In this case, the calculated spectrum is exactly equal to the continuous-time Fourier transform, which consists of discrete components in the frequency domain and corresponds to the Fourier series of that signal.

Next, the relevant frequencies are selected by frequency-domain windowing, using a rectangular window, that is, the spectrum is set to zero at all but the selected frequencies, which corresponds to frequency-domain data filtering. The selected spectrum is then multiplied by the continuous-time frequency response of a pure single and double differentiator to obtain velocity and acceleration estimates. That is, the spectrum is multiplied by $j\omega(k)$ and $-\omega(k)^2$, respectively, where $\omega(k) = 2\pi kf_s/P$, P is the number of samples of the signal, and k is the set of indices of selected frequencies in the discrete spectrum (discrete Fourier transform). The resulting spectrum is then transformed back to the time domain using the inverse discrete Fourier transform. Figure 3 illustrates this operation for velocity estimation. This frequency-domain data filtering, which is also applied to the position measurements, removes the noise from all but the selected frequencies, yielding accurate, for practical purposes noise-free, position, velocity, and acceleration signals. The results are not perfectly free of noise because noise cannot be removed from the selected frequencies.

PARAMETER ESTIMATION AND MODEL VALIDATION

The selection of a parameter-estimation method is a compromise between accuracy and complexity of implementation. Linear least squares parameter estimation (LLSE), which sits at one side of this spectrum, is a non-iterative method that finds the parameter estimates in a single step using the singular value decomposition. LLSE does not discriminate between accurate and inaccurate data, and thus yields biased estimates with non-minimal uncertainty.



FIGURE 4 A KUKA IR 361 industrial robot in the robotics laboratory at KU Leuven. The position controller of the robot is provided by Orocó software [24], [25]. This software facilitates the application of periodic commanded trajectories, while synchronizing encoder and actuator current measurements.

The maximum likelihood estimation sits at the other side of the spectrum since it provides unbiased estimates with minimal uncertainty regardless of the spectrum of the measurement noise. The maximum likelihood estimate of the parameter vector θ is the value of θ that maximizes the likelihood of the measurements. This criterion, which is a nonconvex function of the unknown model parameters, depends on the covariance of the noise on all measurements and derived variables such as joint velocities and accelerations. Solving this nonlinear least squares optimization problem is often cumbersome because it requires an initial guess of the parameters and because it might converge to a local optimum, yielding a suboptimal solution that may be biased.

When the joint position, velocity, and acceleration data are free of noise, which is for practical purposes realized by applying the above-mentioned signal processing, the identification matrix Φ in (2) is free of noise, and the maximum likelihood estimation simplifies to weighted linear least squares estimation (WLSE). The complexity of WLSE is comparable to that of LLSE, in fact, the only difference is that WLSE weighs the data with the inverse of the covariance of the actuator torque measurement noise and there-

An objective of offline programming is to minimize the cycle time of a robot task, since shorter cycle times lead to higher productivity.

TABLE 1 Comparison of actuator torque prediction errors with the measurement noise level. The root mean square of the actuator torque prediction errors is comparable to the standard deviation of the noise on the averaged actuator torque measurements.

	Joint 1	Joint 2	Joint 3
RMS of the prediction error noise level	6.1 N-m 3.3 N-m	6.3 N-m 4.6 N-m	2.9 N-m 1.5 N-m

fore discriminates between accurate and inaccurate data. WLSE has the same favorable properties as the maximum likelihood estimation.

The weighted least squares estimate of the model parameters θ is

$$\hat{\theta}_{WLS} = (\mathbf{F}^T \Sigma^{-1} \mathbf{F})^{-1} \mathbf{F}^T \Sigma^{-1} \tau \quad (7)$$

$$= (\Sigma^{-1/2} \mathbf{F})^+ \Sigma^{-1/2} \tau, \quad (8)$$

where $(\cdot)^+$ denotes the pseudoinverse,

$$\mathbf{F} = \begin{bmatrix} \Phi(q_{t_1}, \dot{q}_{t_1}, \ddot{q}_{t_1}) \\ \vdots \\ \Phi(q_{t_K}, \dot{q}_{t_K}, \ddot{q}_{t_K}) \end{bmatrix}, \quad (9)$$

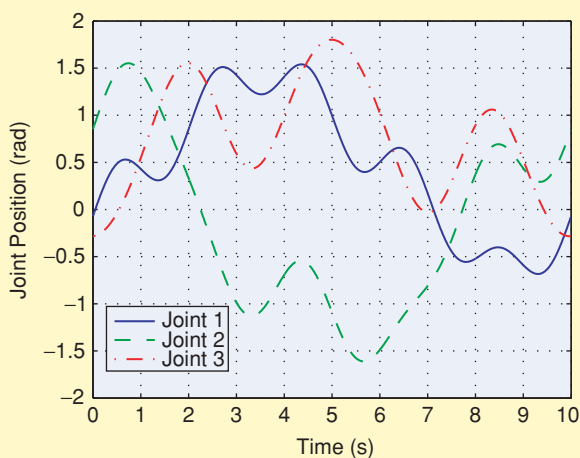


FIGURE 5 Optimized robot-excitation trajectory. One period of the optimized joint trajectories is shown. These trajectories consist of a five-term Fourier series with a base frequency of 0.1 Hz. The trajectory parameters are optimized according to the d -optimality criterion, taking into account workspace limitations, constraints on joint velocities, and accelerations. The optimization criterion is a measure of the size of the overall uncertainty region of the parameter estimates.

and

$$\tau = \begin{bmatrix} \tau_{t_1} \\ \vdots \\ \tau_{t_K} \end{bmatrix}. \quad (10)$$

Here, $\Phi(q_{t_k}, \dot{q}_{t_k}, \ddot{q}_{t_k})$ and τ_{t_k} , for $k = 1, \dots, K$, are the identification matrix and torque vector evaluated using the joint position, velocity, and acceleration data, as well as the actuator torque data at the discrete-time instant t_k . Furthermore, Σ is the covariance matrix of the actuator torque data, which is a dense matrix if the noise is correlated. Here, the assumption is made that the noise is white, which is made for convenience. Since the matrix \mathbf{F} in (9) is free of noise, the parameter estimates are unbiased even if the actual noise is colored, although the estimates may have nonminimal uncertainty [23, pp. 92–106].

The covariance matrix of the estimated parameter vector $\hat{\theta}_{WLS}$ is

$$\mathbf{C} = (\mathbf{F}^T \Sigma^{-1} \mathbf{F})^{-1}, \quad (11)$$

which, along with the related uncertainty bounds on the parameters, can be used for model validation.

The aim of the model-validation step is to obtain confidence in the estimated robot model in view of its intended application. Obviously, the most appropriate validation test is to use the model in the application and evaluate its success. This validation method, however, can lead to undesirable and even dangerous situations. Therefore, validation must be addressed prior to the actual application. Given this requirement, a validation test must evaluate the properties of the estimated model and the parameter estimates that are relevant to the intended application. Unsatisfactory validation leads to a reconsideration of some previous steps of the identification procedure, for instance, a new experiment design or a more elaborate dynamic model.

We consider two model-validation measures, the actuator torque-prediction accuracy and the parameter-estimation accuracy.

Actuator Torque-Prediction Accuracy

The actuator torque-prediction accuracy of a robot model is needed for offline programming, task optimization, and advanced robot control. The robot model (2) is evaluated for some desired motion, described by a set of joint positions q , velocities \dot{q} , and accelerations \ddot{q} ,

yielding actuator torque predictions τ . The same motion is executed by the robot. The actuator torques are measured and compared with the predicted actuator torques. The difference between predicted and measured torque, that is, the prediction error, is expected to be small compared to the torque signal and preferably comparable to the noise level on the actuator torque measurements.

Good validation practice requires that the validation trajectories be different from the excitation trajectory, while being representative of the intended application. For example, robot trajectories for painting and laser cutting applications are smooth and continuous in time, while applications such as pick and place and spot welding are characterized by trajectories with many starts and stops.

Parameter Accuracy

An alternative method for validating the model is to check the accuracy of the estimated parameters. Two approaches are possible. The estimated parameters are compared with an estimate of their confidence interval, or with estimates available from other sources, for example, CAD data of robot parts.

Based on the parameter covariance matrix (11), it is possible to derive confidence intervals for each parameter. Comparison of the parameter values with their confidence interval gives an indication of the accuracy of the individual parameters. If this parameter covariance matrix is not available, an estimate of the parameter uncertainty can still be obtained by repeating the parameter estimation for different excitation trajectories. Subsequently, the mean value of the model parameters and their sample variance can be calculated. This approach is more time consuming than the confidence interval approach but is more reliable.

EXPERIMENTAL RESULTS ON AN INDUSTRIAL ROBOT MANIPULATOR

This section discusses experimental results of the robot identification procedure applied to the first three links of an industrial KUKA IR 361 robot.

Description of the Experimental Setup

The KUKA IR 361, shown in Figure 4, is a six-degree-of-freedom industrial robot manipulator with a payload capacity of 8 kg. Only the first three links are considered here.

A fundamental frequency of 0.1 Hz is selected for the excitation trajectories, resulting in a period of 10 s. The commanded trajectories are five-term Fourier series, involving 11 trajectory parameters for each joint, and a 0.5-Hz bandwidth. Optimization of the trajectory parameters is based on the d -optimality criterion. Figure 5 shows the optimized trajectory for the three robot joints, while Figure 6 shows a three-dimensional representation of this optimized trajectory in the workspace of the robot. The

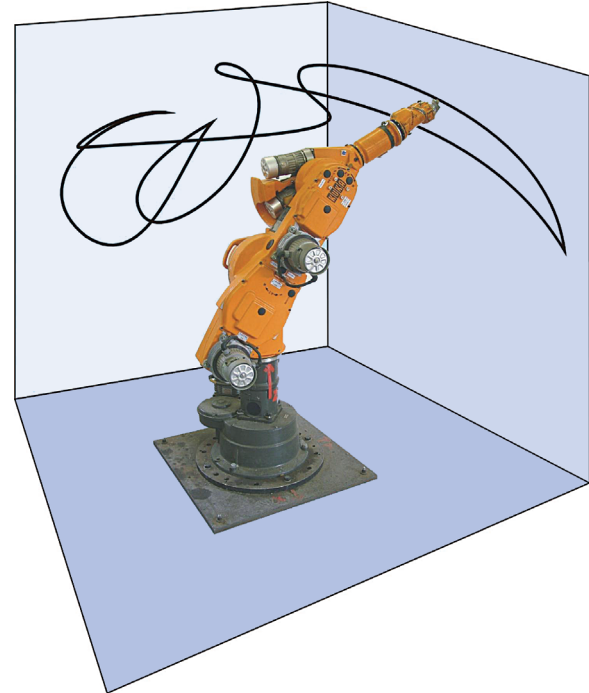


FIGURE 6 Three-dimensional visualization of the optimized excitation trajectory. The curve shows the trajectory of the robot tool center point of the KUKA IR 361 robot. Only the first, second, and third links of the robot are used in this experiment. The robot model identification is based on joint-angle and actuator-torque data measured during successive repetitions of the trajectory.

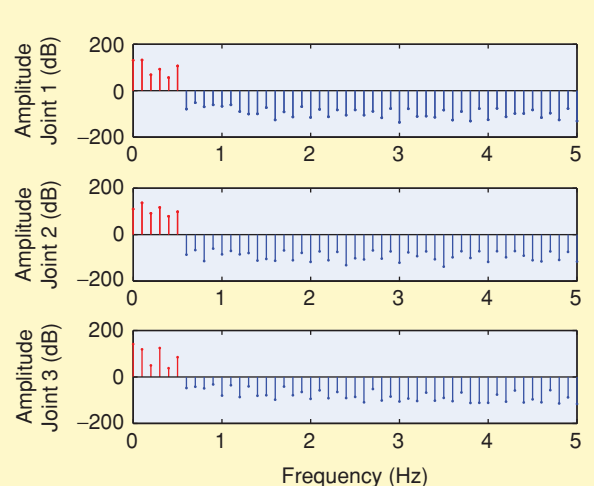


FIGURE 7 Amplitude of the frequency spectrum of one period of the measured joint trajectories. These signals have a base frequency of 0.1 Hz and contain five dominant harmonics, in accordance with the commanded trajectories. The amplitudes of the higher frequency components are significantly smaller than the five low-frequency components, which shows that the measurement noise and tracking errors caused by the limited bandwidth of the robot controller are small. During the signal processing step, only the first five frequencies are selected. By ignoring the higher frequencies, for practical purposes noiseless joint position signals are obtained.

TABLE 2 Model validation based on actuator torque prediction for the validation trajectory. The RMS of the actuator torque prediction errors is small compared to the actuator torques, which indicates that the identified model can accurately predict the actuator torques for point-to-point motions. These motions are typical of pick-and-place and spot-welding operations.

	Joint 1	Joint 2	Joint 3
RMS of the prediction error	8.9 N-m	11.8 N-m	4.4 N-m

trajectories are implemented on the Orocosp [24], [25] control platform, which replaces the standard industrial position controller for this robot. After the transients die out, the joint positions and motor currents of the first three robot joints are measured. The total measurement time is 160 s, corresponding to 16 periods of the excitation trajectory. The data sampling rate is 150 Hz. Figure 7 shows the frequency spectrum of one period of the joint trajectories measured during the robot-excitation experiment.

Parameter Estimation

The robot model for the first three links contains 15 barycentric parameters, six friction parameters (viscous and Coulomb friction parameters for each joint), and two additional parameters that model the gravity-compensating spring. The rotor inertia of the actuator for the third axis is added as an extra parameter to account for the coupling effect introduced by the mounting of the third actuator on the second link [12]. These model parameters are estimated using the robot identification procedure discussed above.

Figure 8 compares the averaged measured torques for the excitation trajectory with the predicted actuator torques based on the identified model parameters and the available motion data. The third column shows that the prediction error is small, except during velocity reversal due to the limited accuracy of the friction model at low velocities. Table 1 compares the RMS of the prediction errors with the standard deviation of the noise on the averaged actuator torque measurements.

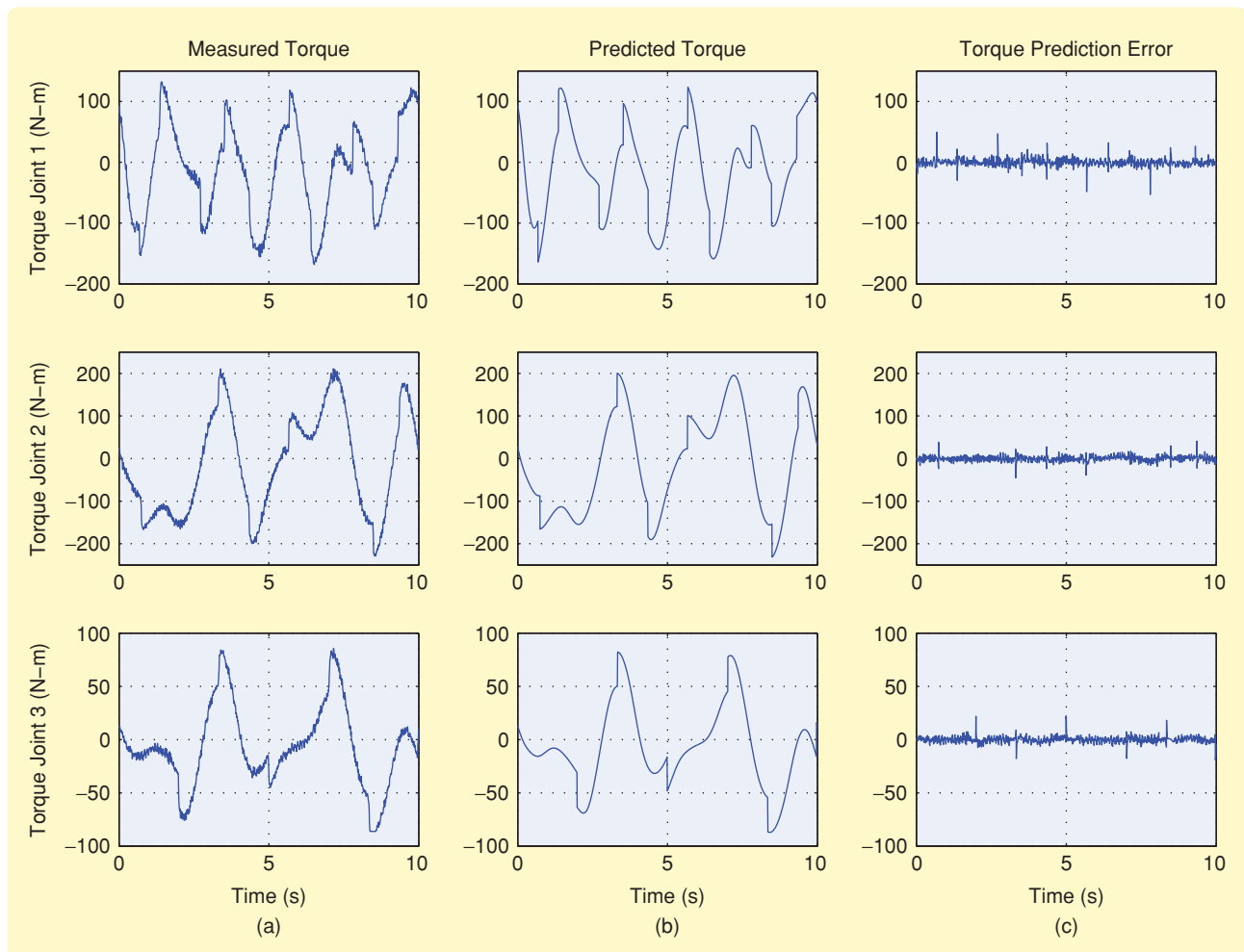


FIGURE 8 Model validation based on actuator torque prediction for the excitation trajectory. The predicted actuator torques of the first three joints of the KUKA IR 361 robot are compared with the averaged measured torques for the excitation trajectory. (c) shows that the prediction errors are small. The remaining peaks occur during velocity reversal, indicating that the friction model cannot capture the complex dynamic friction behavior at low velocities.

Validation Experiment

For validation, we choose a trajectory that is representative for pick-and-place as well as spot-welding operations. This trajectory (see Figure 9) consists of point-to-point motions between 20 randomly chosen points in the robot workspace. The robot moves with maximum acceleration and deceleration between these points, resulting in a trapezoidal velocity profile between two successive points, and comes to rest with zero dwell time at each point.

Figure 10 shows the measured and predicted actuator torques and the corresponding prediction errors. Comparison of the prediction errors with the measured torques shows that the model we obtain is capable of accurately predicting the actuator torque data. The peaks in the prediction error indicate again that the assumed friction model, which includes viscous and Coulomb friction only, is unable to capture the complex dynamic friction behavior. Table 2 shows the RMS of the actuator torque prediction errors for this validation experiment. Extending the robot model to include more advanced friction models, as well as models of the mechanical losses in the actuators and the efficiency of the transmissions, further improves the prediction accuracy [26]. These model extensions are, however, nonlinear in the parameters, and thus considerably complicate parameter estimation.

INDUSTRIAL APPLICATION: ROBOT PAYLOAD IDENTIFICATION

As industrial robot manipulators evolve toward more lightweight structures, the contribution of the payload to the required actuator torques increases [27]. As a consequence, accurate knowledge of the payload inertial parameters is a prerequisite for task optimization and model-based robot control. These payloads consist of parts from multiple manufacturers, which are assembled in various configurations.

A payload identification module based on periodic excitation is available as a plug-in for KUKA robot controllers. Payload identification is typically performed on the shop floor by the robot operator before operation begins with a chosen tool. These conditions impose an additional requirement on the identification module, specifically, the workspace, being inside the production line, is much more restricted than for a general robot identification experiment.

To fulfill this additional requirement, identification of the complete robot including the payload is avoided by using estimates of the robot link inertial parameters as a priori information. This approach reduces the number of unknown parameters in the identification model considerably, which helps to reduce the uncertainty on the parameter estimates for a given data set [19].

More importantly, the experiment design can now focus on finding a trajectory that provides optimal excitation for the payload parameters rather than for all robot inertial parameters. Good excitation of all robot dynamics

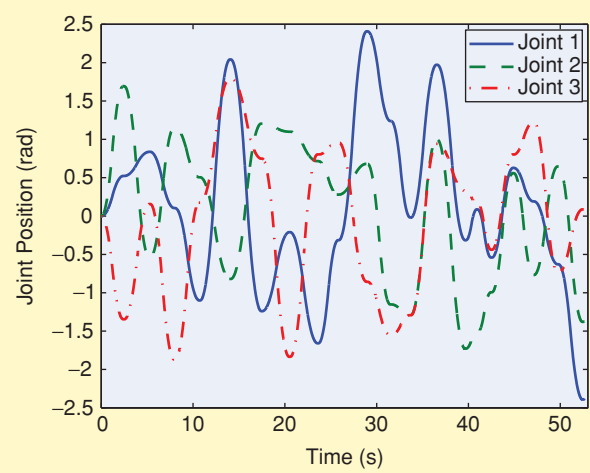


FIGURE 9 Robot model validation trajectory. The trajectory consists of point-to-point motions between 20 randomly chosen points in the robot workspace. The robot moves with maximum acceleration and deceleration between these points, and comes to rest with zero dwell time at each point. This validation trajectory is representative of pick-and-place and spot-welding operations.

is usually not feasible inside a production line, yielding inaccurate parameter estimates.

Identification Procedure

Modeling

The derivation of the payload identification model starts from the observation that the robot links and the payload each contribute separately to the joint torques, that is,

$$\tau = \tau_{\text{robot links}} + \tau_{\text{payload}} \quad (12)$$

$$= \Phi(q, \dot{q}, \ddot{q})\theta + \Phi_L(q, \dot{q}, \ddot{q})\theta_L, \quad (13)$$

where Φ_L is the payload identification matrix, and θ_L is a vector that contains the barycentric parameters of the payload. These barycentric parameters contain the payload mass as well as the first- and second-order moments with respect to the last robot rotation axis. Since the robot payload is the last body in the serial robot structure, an unambiguous transformation exists between the barycentric parameters of the payload and its classical inertia parameters.

The first term in (13), which corresponds to (2), describes the robot dynamics. This term represents the actuator torque contributions that result from the inertial parameters, possibly gravity-compensating springs, and joint friction. The first two contributions do not change by adding a payload to the robot. Therefore, the corresponding parameter set is considered as a priori information for the robot payload identification. The joint friction changes with the payload, and, consequently, the parameters are re-estimated. Altogether, the number of unknown parameters

remains small, which is beneficial for the robustness and accuracy of the payload parameter estimation.

Excitation Trajectory

An excitation trajectory that is optimal for payload identification is quite different from the trajectories used for robot identification. This difference is explained as follows. The inertial parameters of the base links, which are in most cases the first three links, dominate the dynamics of the robot. Therefore, trajectory optimization for robot identification typically yields fast motions for the base joints. On the other hand, accurate estimation of the inertial parameters of the payload requires fast payload motions, which are easily accomplished using the robot wrist joints and one additional base joint. Moreover, the workspace available for performing the experiments is often more limited for payload than for robot identifica-

tion, because the former is most often performed inside a production line.

Signal Processing and Parameter Estimation

The signal processing and parameter estimation steps of the payload identification procedure use the same algorithms as the general robot identification procedure. Hence the payload identification procedure benefits from the advantages associated with periodic excitation. In addition, the smaller set of unknown parameters results in faster convergence and more accurate parameter estimates.

Description of the Experimental Setup

The test setup consists of a six-degree-of-freedom KUKA KR 15 industrial manipulator (Figure 11) equipped with a payload. The KUKA KR15 is an industrial robot with a PC-based

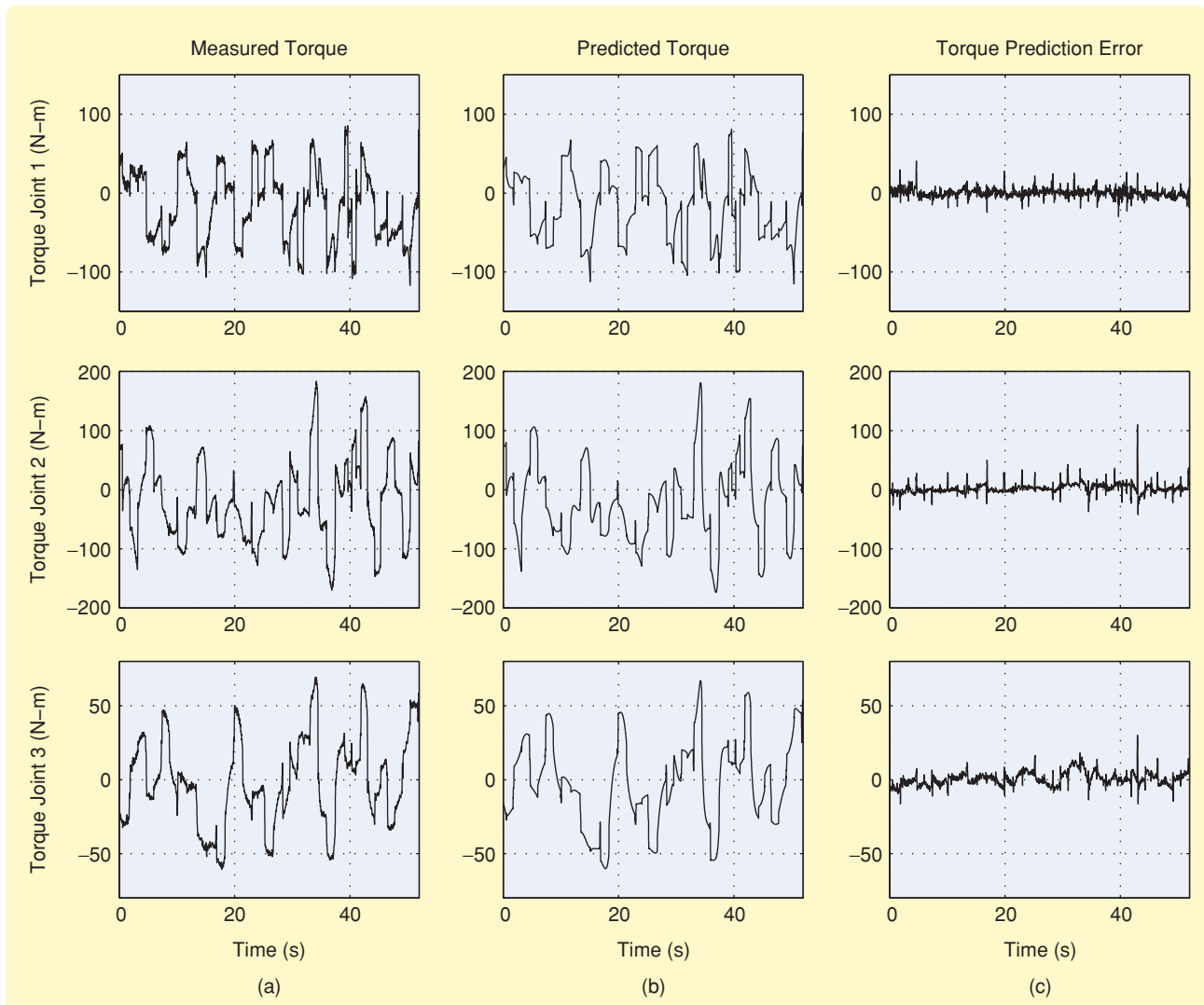


FIGURE 10 Model validation based on actuator torque prediction for the validation trajectory. The predicted actuator torques of the first three joints of the KUKA IR 361 robot are compared with the measured torques for the validation trajectory. Part (c) shows that the prediction errors are small. These small prediction errors show that the estimated robot model can accurately predict the actuator torques, and is thus well suited for model-based robot control and dynamic task optimization.

controller and a payload capacity of 15 kg. To validate the accuracy of the payload identification method, a calibrated reference payload is used, shown in Figure 12. A detailed CAD model provides estimates of all ten inertial parameters of this payload. These values are used as reference values for the robot payload identification experiment presented here and are shown in the second column of Table 3.

The robot excitation is limited to the last four joints of the manipulator. A fundamental frequency of 0.033 Hz is selected for the excitation trajectories, consisting of the fundamental frequency and its 20th or 25th harmonic. These choices for the robot excitation are imposed by the payload identification plug-in of the robot controller. The data are sampled with a sampling period of 12 ms.

Parameter Estimation and Experimental Results

The payload identification model contains 18 identifiable parameters, this is, the ten inertial parameters of the payload as well as eight friction parameters. The friction parameters consist of one Coulomb and one viscous friction parameter for each of the last four joints. Experimental experience shows that the friction changes significantly

TABLE 3 Validation of the accuracy of the inertial parameter estimates for the reference payload shown in Figure 12. The reference values of the inertial parameters result from a CAD model of the payload. Ten experiments with the same payload, each using a different excitation trajectory, are performed. From the resulting ten sets of parameter estimates, the mean value and standard deviation are calculated, given in the third and fourth columns, respectively. All reference values lie within the 2σ confidence interval of the mean estimated values.

Parameter	Reference Value	Mean Value	Standard Deviation
m (kg)	9.579	9.618	0.174
c_x (m)	0.024	0.0246	0.0010
c_y (m)	0.090	0.0930	0.0016
c_z (m)	-0.202	-0.2065	0.0064
I_{xx} (kg·m ²)	0.612	0.677	0.077
I_{yy} (kg·m ²)	0.063	0.121	0.077
I_{zz} (kg·m ²)	0.637	0.621	0.020
I_{xy} (kg·m ²)	-0.158	-0.164	0.011
I_{xz} (kg·m ²)	-0.002	-0.004	0.010
I_{yz} (kg·m ²)	-0.008	-0.010	0.016

with the payload of the robot. A re-identification of the friction parameters is therefore necessary to obtain accurate parameter estimates.

Ten identification experiments are performed. Each experiment uses a different excitation trajectory and yields a set of parameter estimates based on data measured during ten periods. Based on the resulting ten sets of parameter estimates, mean parameter values and their standard deviation are calculated. The results are presented in Table 3 and compared with the reference values. The reference values lie within the 2σ confidence interval around the average parameter estimates.



FIGURE 11 The KUKA KR 15 industrial robot in the robotics laboratory at KU Leuven with a reference payload. The KUKA KR 15 is a six-degree-of-freedom industrial robot with a PC-based controller and a payload capacity of 15 kg. A software plug-in makes it possible to perform robot payload identification experiments that use periodic trajectories for the last four robot axes, that is, the elbow and wrist axes.

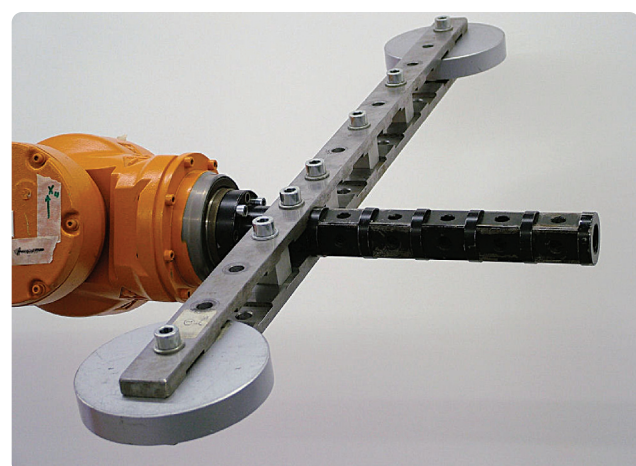


FIGURE 12 The reference payload used to validate the payload identification procedure. This payload is reconfigurable. For example, its mass and principal moments of inertia can be changed between 1.4 and 15 kg and from nearly zero to 3 kg·m², respectively. The reference values for the inertia parameters are calculated from a CAD model. The second column of Table 3 shows these reference values for the configuration of the payload shown here.

The use of periodic excitation is the key feature of the robot identification method.

Figure 13 evaluates the model accuracy based on its actuator torque prediction accuracy for a validation trajectory. The torque prediction error is small except during velocity reversals, as expected.

The accuracy of the parameter estimates and the actuator torque prediction satisfy the requirements imposed by industry. The mass of a payload can be estimated within 5% and its center of mass within 1 cm.

CONCLUSIONS

The use of periodic excitation is the key feature of the presented robot identification method. Periodic excitation

allows us to integrate the experiment design, signal processing, and parameter estimation. This integration simplifies the identification procedure and yields accurate models. Experimental results on an industrial robot manipulator show that the estimated dynamic robot model can accurately predict the actuator torques for a given robot motion. Accurate actuator torque prediction is a fundamental requirement for robot models that are used for offline programming, task optimization, and advanced model-based control.

A payload identification approach is derived from the integrated robot identification method, and possesses the same favorable properties.

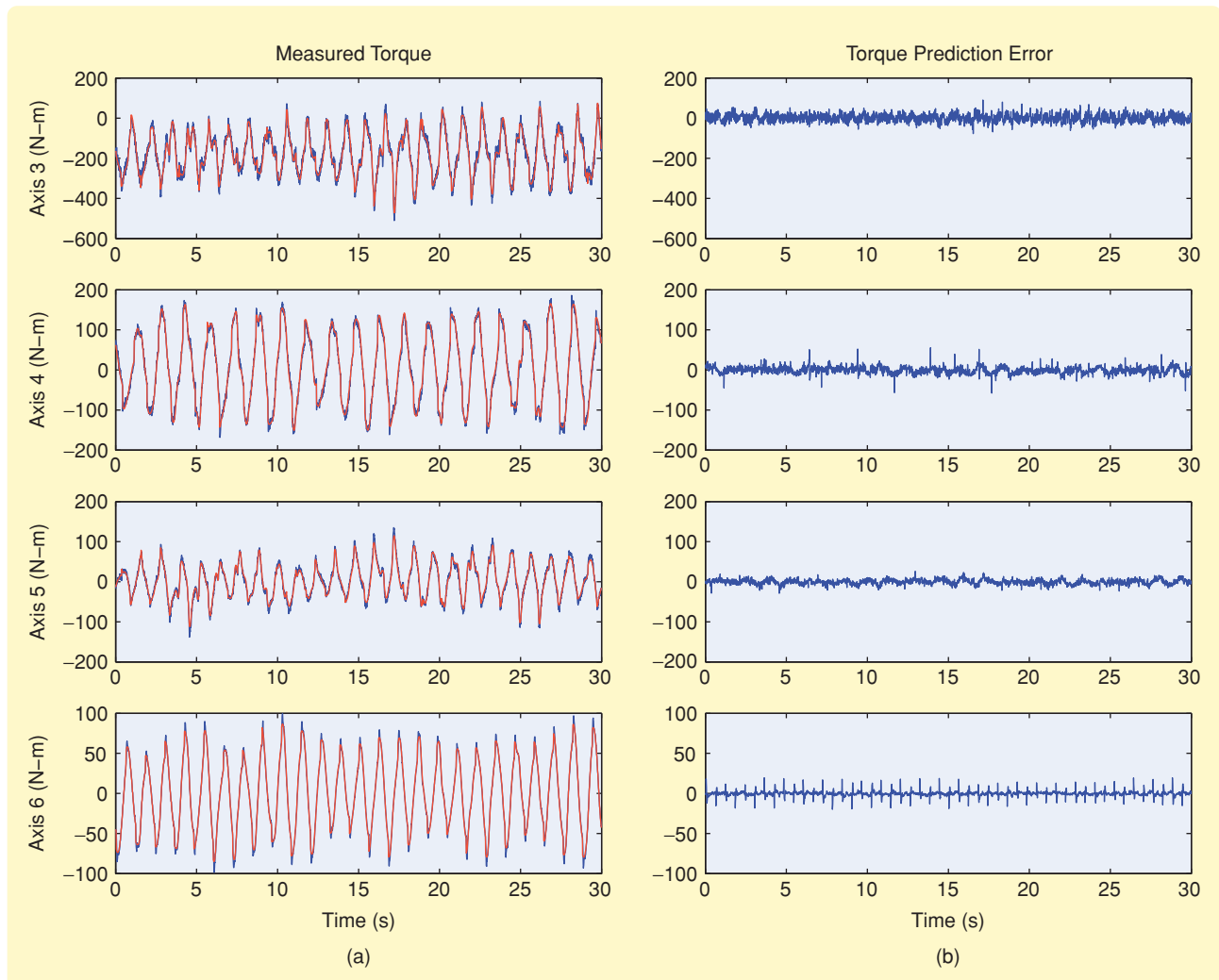


FIGURE 13 Model validation based on actuator torque prediction for the validation trajectory. The predicted actuator torques of joints three to six of the KUKA KR 15 robot with reference payload are plotted with the measured torques in (a). (b) shows that the prediction errors are small.

ACKNOWLEDGMENTS

This article presents research results of the K.U. Leuven Concerted Research Action GOA/05/10. The work is also sponsored by a specialization grant of the Institute for the Promotion of Innovation through Science and Technology in Flanders (IWT-Vlaanderen), by the Research Council K.U.Leuven, CoE EF/05/006 Optimization in Engineering (OPTEC), and by the Belgian Network Dynamical Systems, Control, and Optimization, funded by the Interuniversity Attraction Poles Programme, initiated by the Belgian State, Science Policy Office. The scientific responsibility rests with its authors.

REFERENCES

- [1] "RRS robot controller simulation (RCS) interface," Berlin, 2001. [Online]. Available: <http://www.realistic-robot-simulation.org>
- [2] J.Y.S. Luh, M.W. Walker, and R.P. Paul, "On-line computational scheme for mechanical manipulators," *J. Dynamic Syst., Measure. Control*, vol. 102, no. 2, pp. 69–76, June 1980.
- [3] J.-J.E. Slotine, "The robust control of robot manipulators," *Int. J. Robot. Res.*, vol. 4, no. 2, pp. 49–64, 1985.
- [4] P. Khosla and T. Kanade, "Experimental evaluation of nonlinear feedback and feedforward control schemes for manipulators," *Int. J. Robot. Res.*, vol. 7, no. 1, pp. 18–28, Feb. 1988.
- [5] C. Canudas de Wit, B. Siciliano, and G. Bastin, *Theory of Robot Control*. New York: Springer-Verlag, 1996.
- [6] F. Caccavale and P. Chiacchio, "Identification of dynamic parameters and feedforward control for a conventional industrial manipulator," *Control Eng. Practice*, vol. 2, no. 6, pp. 1039–1050, 1994.
- [7] M. Olsen, J. Swevers, and W. Verdonck, "Maximum likelihood identification of a dynamic robot model: Implementation issues," *Int. J. Robot. Res.*, vol. 21, no. 2, pp. 89–96, Feb. 2002.
- [8] C. Atkeson, C. An, and J. Hollerbach, "Estimation of inertial parameters of manipulator loads and links," *Int. J. Robot. Res.*, vol. 5, no. 3, pp. 101–119, 1986.
- [9] P. Fisette, B. Raucourt, and J.-C. Samin, "Minimal dynamic characterization of tree-like multibody systems," *Nonlinear Dynamics*, vol. 9, no. 1–2, pp. 165–184, 1996.
- [10] L. Ljung, *System Identification: Theory for the User*. Englewood Cliffs, New Jersey: Prentice-Hall, 1987.
- [11] M. Renaud, "Quasi-minimal computation of the dynamic model of a robot manipulator utilizing the Newton-Euler formalism and the notion of augmented body," in *Proc. IEEE Int. Conf. Robot. Automation*, Raleigh, North Carolina, 1987, pp. 1677–1682.
- [12] L. Sciavicco, B. Siciliano, and L. Villani, "Lagrange and Newton-Euler dynamic modelling of a gear-driven rigid robot manipulator with inclusion of motor inertia effects," *Advanced Robotics*, vol. 10, no. 3, pp. 317–334, 1996.
- [13] W. Khalil and E. Dombre, *Modeling, Identification and Control of Robots*. London: Hermes Penton Ltd, 2002.
- [14] J. Swevers, F. Al-Bender, C. Ganseman, and T. Prajogo, "An integrated friction model structure with improved presliding behavior for accurate friction compensation," *IEEE Trans. Automat. Contr.*, vol. 45, no. 4, pp. 675–686, 2000.
- [15] F. Al-Bender, V. Lampaert, and J. Swevers, "The generalized Maxwell-slip model: A novel model for friction simulation and compensation," *IEEE Trans. Automat. Contr.*, vol. 50, no. 11, pp. 1883–1887, Nov. 2005.
- [16] M. Daemi and B. Heimann, "Identification and compensation of gear friction for modeling of robots," in *Proc. 11th CISM-IFTOMM Symp. Theory and Practice Robots and Manipulators*, Udine, Italy, 1996, pp. 89–96.
- [17] B. Armstrong, "On finding exciting trajectories for identification experiments involving systems with nonlinear dynamics," *Int. J. Robot. Res.*, vol. 8, no. 6, pp. 28–48, 1989.
- [18] M. Gautier and W. Khalil, "Exciting trajectories for the identification of base inertial parameters of robots," *Int. J. Robot. Res.*, vol. 11, no. 4, pp. 362–375, 1992.
- [19] R. Pintelon and J. Schoukens, *System Identification: A Frequency Domain Approach*. New York: Wiley, 2001.
- [20] M. Gautier, "Identification of robots dynamics," in *Proc. IFAC Symp. Theory Robots*, Vienna, Austria, 1986, pp. 351–356.
- [21] J. Swevers, B. Naumer, S. Pieters, E. Biber, W. Verdonck, and J. De Schutter, "An experimental robot load identification method for industrial application," in *Advanced Robotics: Experimental Robotics VIII*, New York: Springer-Verlag, 2003, pp. 318–327.
- [22] P. Corke, "In situ measurement of robot motor electrical constants," *Robotica*, vol. 14, no. 4, pp. 433–436, 1996.
- [23] J.P. Norton, *An Introduction to Identification*. London: Academic, 1986.
- [24] H. Bruyninckx, (2001) "Open Robot Control Software," Leuven, Belgium. [Online]. Available: <http://www.orocos.org/>
- [25] P. Soetens and H. Bruyninckx, "Realtime hybrid task-based control for robots and machine tools," in *Proc. IEEE Int. Conf. Robot. Automation*, Barcelona, Spain, 2005, pp. 260–265.
- [26] J. Swevers, W. Verdonck, B. Naumer, S. Pieters, and E. Biber, "An experimental robot load identification method for industrial application," *Int. J. Robot. Res.*, vol. 21, no. 8, pp. 701–712, 2002.
- [27] G. Hirzinger, N. Sporer, A. Albu-Schäffer, M. Hähnle, R. Krenn, A. Pascucci, and M. Schedl, "DLR's torque-controlled light weight robot III—Are we reaching the technological limits now?" in *Proc. IEEE Int. Conf. Robot. Automation*, Washington DC, 2002, pp. 1710–1716.

AUTHOR INFORMATION

Jan Swevers (jan.swevers@mech.kuleuven.be) received the M.Sc. degree in electrical engineering and the Ph.D. degree in mechanical engineering from the Katholieke Universiteit Leuven, Belgium, in 1986 and 1992, respectively, where he is currently a professor in the Department of Mechanical Engineering, Division of Production Engineering, Machine Design and Automation (PMA). His research interests include modeling, identification, and control of mechatronic systems. He can be contacted at the Department of Mechanical Engineering, Division PMA, Katholieke Universiteit Leuven, Celestijnenlaan 300 B, B-3001 Heverlee, Belgium.

Walter Verdonck received the M.Sc. degree in mechanical engineering and the Ph.D. degree in mechanical engineering from the Katholieke Universiteit Leuven, Belgium, in 1999 and 2004, respectively. He is currently employed as a research engineer at the Flanders' Mechatronics Technology Centre. His research interests include modeling, identification, and control of robots and mechatronic systems.

Joris De Schutter received the M.Sc. degree in mechanical engineering and the Ph.D. degree in mechanical engineering from the Katholieke Universiteit Leuven, Belgium, in 1980 and 1986, respectively, as well as an M.Sc. degree from M.I.T. in 1981. He is currently full professor in the Department of Mechanical Engineering, Division of Production Engineering, Machine Design and Automation at K.U. Leuven. His research interests include programming and control of sensor-based robots, as well as optimal design and control of high performance mechanical and mechatronic drive systems.

